Inorganic Chemistry

ARTICLE

pubs.acs.org/IC

A Turn-on Fluorescent Iron Complex and Its Cellular Uptake

Jy D. Chartres,[†] Michael Busby,[‡] Mark J. Riley,[†] Jason J. Davis,[*,‡] and Paul V. Bernhardt[*,†]

[†]School of Chemistry and Molecular Biosciences, University of Queensland, Brisbane, Queensland, Australia 4072

[‡]Physical and Theoretical Chemistry Laboratory, University of Oxford, South Parks Road, Oxford, OX1 3QZ, United Kingdom

Supporting Information

ABSTRACT: In the treatment of chronic iron overload disorders, ligands capable of complexing so-called "labile" (nonprotein bound) Fe are required to enter iron-loaded cells, sequester excess Fe, and then exit the cell (and the body) as an intact Fe complex. Despite the emergence of several ligand families that show high activity in mobilizing intracellular Fe, the mechanism and the locations of these subcellular labile Fe pools are still poorly understood. Our previous studies have unearthed a class of heterocyclic hydrazine-based chelators (e.g., benzoyl picolinoyl hydrazine, H_2BPH) that show excellent activity at mobilizing Fe from Fe-loaded cells. Herein, we have grafted a fluorescent tag (rhodamine B) onto H_2BPH to generate a ligand (L^1) that is nonfluorescent in its uncomplexed form but becomes strongly fluorescent in complex with Fe^{III}. The free ligand and its 1:2 Fe complex $[Fe^{III}(L^1)_2]^{3+}$ have both been fully characterized spectroscopically and with X-ray crystallography. Confocal fluorescent microscopy of HeLa cells incubated with $[Fe^{III}(L^1)_2]^{3+}$ shows that the complex rapidly enters HeLa cells and localizes within endosomes/lysosomes.

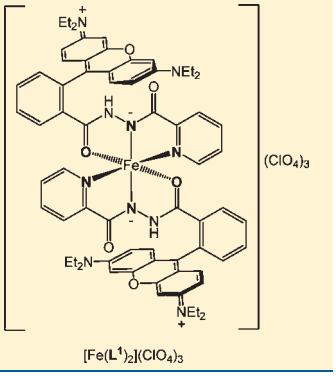

$[Fe(L^1)_2](ClO_4)_3$

INTRODUCTION

Iron overload disorders are potentially life threatening medical conditions.[1−3] In cases of acute Fe overload, resulting from frequent blood transfusions, administration of Fe chelators is necessary to enable excretion of this element.[4,5] In previous studies, we have identified a number of ligands with potential applications in Fe chelation therapy (e.g., H_2BPH in Scheme 1).[6−8] This and other structurally related ligands are very active in mobilizing intracellular Fe, yet they do not compete directly with Fe binding proteins such as the serum Fe transporter, transferrin. In fact, little is known about the mechanism by which these chelators access Fe or where they localize intracellularly.

The fluorescence imaging of metal ions *in vivo* is a rapidly growing and important field,[9−13] and careful design of ligands has enabled the mapping of cellular concentrations of a number of different metal ions. Several reported fluorescent probes (e.g., calcein,[14] phen green SKA,[15] and hydroxypyridinones[13]) have been utilized to quantify labile Fe pool concentrations in cells. However, these approaches are problematic as they are based on *quenching* the fluorescence of a free ligand upon complexation with Fe (i.e., a "turn-off" sensor). Unless quenching is complete, quantification, or even the observation of significant changes in fluorescence intensity, becomes problematic. The reverse process of fluorescence "turn-on" from a zero background is experimentally more selective and considerably more definitive. More recently, examples of "turn-on" fluorescent probes for Fe^{III} have been proposed,[16−20] although direct evidence that the fluorescent species *in vivo* is actually an Fe complex has been lacking with no structural characterization of any putative Fe complex.

Herein, we have elaborated upon the hydrazine chelator H_2BPH with a rhodamine B fluorophore to produce a ligand $\mathbf{L^1}$ (Scheme 1) that is fluorescent while bound to Fe^{III} and retains the same *NNO* donor set and basic structure as its parent chelator H_2BPH. As expected from the known chemistry of rhodamine and its analogs,[18] $\mathbf{L^1}$ is typically found in its (spiro) ring-closed form at neutral pH and is nonfluorescent.

Scheme 1

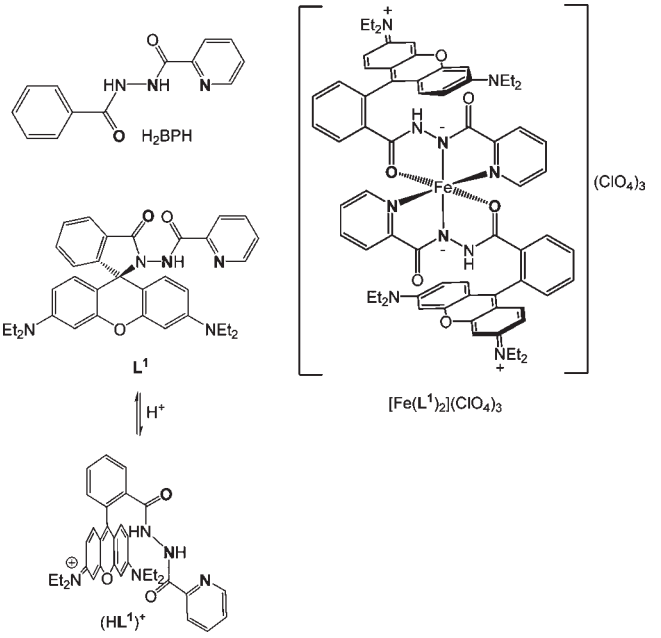

$[Fe(L^1)_2](ClO_4)_3$

Received: July 13, 2011
Published: August 03, 2011

EXPERIMENTAL SECTION

Caution! *Although we have experienced no issues with the compounds prepared, perchlorate salts are potentially explosive and should only be handled in small quantities and should never be heated in the solid state or scraped from sintered glass frits.*

Syntheses. Rhodamine B hydrazide was synthesized using a literature procedure.[21] LysoTracker green was obtained from Molecular Probes (Invitrogen). All other reagents were AR grade.

*N-(3′,6′-Bis(diethylamino)-3-oxospiro[isoindoline-1,9′-xanthen]-2-yl) picolinamide (**L**^{1}).* Picolinic acid (0.74 g, 6.0 mmol) and 1-methylimidazole (1.23 g, 15.0 mmol) were dissolved in MeCN (50 mL), and the mixture cooled to −5 °C. Tosyl chloride (1.14 g, 6.0 mmol) was added, and the reaction mixture was stirred at −5 °C for 30 min. Rhodamine B hydrazide **1** was dissolved in MeCN (50 mL), and the resulting red solution added to the reaction mixture. After warming to room temperature, the reaction mixture was stirred for 16 h. The solvent was evaporated, and the residue dissolved in CH_2Cl_2 (100 mL) before being washed with saturated sodium bicarbonate solution (2 × 150 mL). The organic layer was dried over $MgSO_4$, filtered, and evaporated. The residue was chromatographed on neutral alumina eluting with 0% to 2% $MeOH/CH_2Cl_2$. Ligand **L**^{1} was obtained as a tan colored solid (1.75 g, 62%). Found: C, 72.3; H, 6.28; N, 12.6. $C_{34}H_{35}N_5O_3$ requires: C, 72.7; H, 6.28; N, 12.5). ^{1}H NMR (500 MHz, $CDCl_3$): δ_H 1.15 (t, J = 7 Hz, 12 H, CH_3), 3.32 (m, 8 H, CH_2), 6.3−6.4 (overlapping m, 4 H, H-4′/5′ and H-2′/7′), 6.82 (d, J = 9 Hz, 2 H, H-1′/8′), 7.11 (m, 1 H, isoindoline H-7), 7.34 (m, 1 H, pyridine H-5), 7.47 (m, 2 H, isoindoline H-5 and H-6), 7.73 (m, 1 H, pyridine H-4), 7.97 (m, 1 H, isoindoline H-4), 8.04 (m, 1 H, pyridine H-3), 8.41 (m, 1 H, pyridine H-6), 9.13 (s, 1 H, NH). ^{13}C NMR (100 MHz, $CDCl_3$): δ_C 12.6 (CH_3), 44.3 (CH_2), 66.0 (spiro C), 97.7 (C-2′/7′), 104.5 (C-8a′/9a′), 108.0 (C-4′/5′), 122.8 (pyridine C-3), 123.5 (isoindoline C-4), 123.9 (isoindoline C-7), 126.4 (pyridine C-5), 128.1 (isoindoline C-6), 128.5 (isoindoline C-7a), 129.2 (C-1′/8′), 133.0 (isoindoline C-5), 137.0 (pyridine C-4), 147.9 (pyridine C-6), 148.8 (pyridine C-2), 148.9 (C-3′/6′), 152.4 (isoindoline C-3a), 153.5 (C-4a′/10a′), 161.9 (picolinamide C═O), 165.0 (isoindoline C-3). λ_{max}, nm (ε, M^{-1} cm^{-1}) 239 (48 300), 272 (32 400), 313 (12 100). m/z (ES): 562.3 $(M + H)^+$. A sample of **L**^{1} was dissolved in a minimum amount of EtOAc, and refluxing Et_2O added, which resulted in a precipitate. The suspension was refluxed, and the supernatant decanted. On cooling, colorless crystals suitable for X-ray work formed from the supernatant. These were filtered off and washed with ether before drying under a vacuum. The crystals attained a purple tinge upon exposure to the air.

*[Fe(**L**^{1})$_2$](ClO$_4$)$_3$·3H$_2$O.* To a solution of **L**^{1} (280.8 mg, 0.50 mmol) in EtOH (20 mL) was added a solution of $Fe(ClO_4)_3·6H_2O$ (115.6 mg, 0.25 mmol) in ethanol (10 mL), resulting in a dark red/purple solution. The reaction mixture was refluxed for 30 min and then allowed to stand at room temperature overnight. The resulting solid was filtered off and washed with a minimum amount of EtOH followed by three washings with Et_2O. After drying under vacuum conditions, the complex was obtained as a very dark brown solid (150 mg, 41%). Found: C, 53.2; H, 5.04; N, 9.23. $C_{68}H_{70}N_{10}Cl_3FeO_{18}·3H_2O$ requires: C, 53.3; H, 5.00; N, 9.15). Electronic spectrum (MeCN), λ_{max}, nm (ε, M^{-1} cm^{-1}): 239 (86 400), 271 (sh 57 700), 304 (sh 33 100), 348 (sh 12 200), 554 (50 300), 691 (2700). Crystals of the complex were obtained by vapor diffusion of Et_2O into a MeCN solution of the complex (1 mg/mL).

Crystallography. X-ray data were collected at 293 K using an Oxford Diffraction Gemini CCD diffractometer with Mo Kα radiation. Data reduction was performed with the CrysAllisPro program (Oxford Diffraction vers. 171.34.40). Structures were solved by direct methods with SHELXS86 and refined with SHELX97.[22] The thermal ellipsoid diagrams were produced with ORTEP3[23] rendered with PovRay (version 3.5), and all calculations were performed within the WinGX package.[24] Crystal and refinement data are given in Table 1.

Table 1. Crystal Data

	L^1	$[Fe(L^1)_2](ClO_4)_3·2H_2O$
formula	$C_{34}H_{35}N_5O_3$	$C_{68}H_{74}Cl_3FeN_{10}O_{20}$
fw	561.69	1513.57
cryst syst	triclinic	triclinic
space group	$P\bar{1}$ (No. 2)	$P\bar{1}$ (No. 2)
a/Å	8.9023(8)	14.801(1)
b/Å	12.016(1)	16.137(1)
c/Å	14.510(2)	16.684(1)
α/deg	94.170(8)	76.148(6)
β/deg	95.859(8)	70.432(6)
γ/deg	97.383(8)	89.244(5)
V/Å^3	1525.4(3)	3635.8(4)
Z	2	2
T/K	293(2)	293(2)
λ/Å	0.71073	0.71073
μ/mm^{-1}	0.080	0.396
ρ_{calc}/g cm^{-3}	1.223	1.383
N_{tot}	10538	24923
N_{unique} (R_{int})	5387 (0.066)	12785 (0.149)
N_{obs} (>2σ(I))	1411	2413
R (obs. data)[a]	0.0435	0.0754
wR_2 (all data)[b]	0.0723	0.1961

[a] $R(F_o) = \Sigma||F_o| - |F_c||/\Sigma|F_o|$. [b] $R_w(F_o^2) = [\Sigma w(F_o^2 - F_c^2)/\Sigma wF_o^2]^{1/2}$.

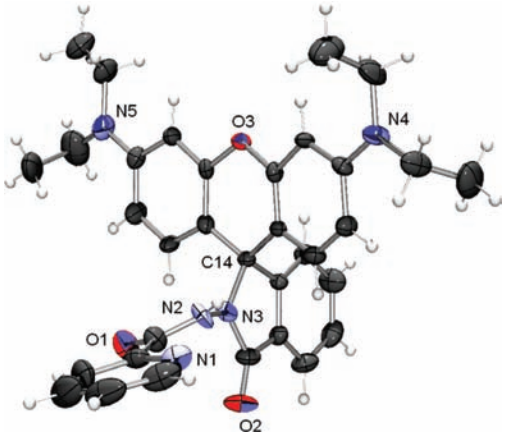

Figure 1. ORTEP view of the spiro (ring-closed) form of **L**^{1} (30% probability ellipsoids) rendered with PovRay (version 3.5). Disorder in one of the ethyl groups not shown for clarity.

There was disorder observed in both structures. One ethyl group in **L**^{1} was found in two different positions that were refined with complementary occupancies. In the structure of $[Fe(L^1)_2](ClO_4)_3·2H_2O$, all three perchlorate anions were disordered. Two anions were rotationally disordered about a common Cl atom, while the third was found in two independent locations. No more than two contributors were refined for each ClO_4^- anion and these were refined with complementary occupancies. No H atoms were located for the water molecules.

Physical Methods. NMR spectra were obtained on a Bruker Avance 500 MHz spectrometer while fluorescence and excitation spectra were measured on a Perkin-Elmer LS50B fluorescence spectrophotometer.

dx.doi.org/10.1021/ic201495r |*Inorg. Chem.* 2011, 50, 9178–9183

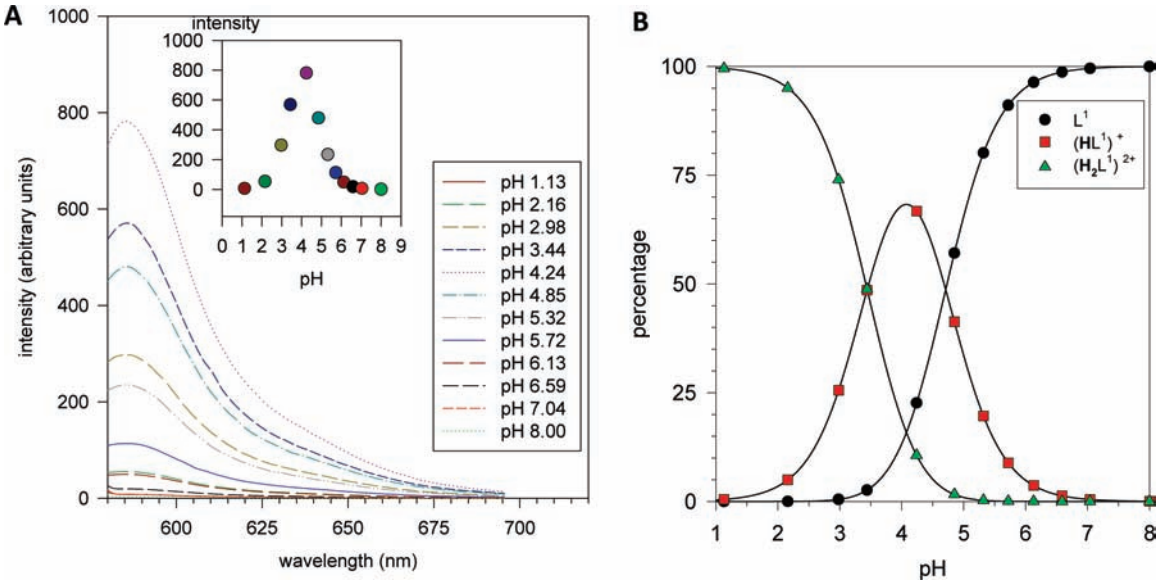

Figure 2. (A) pH-dependent fluorescence spectra of $\mathbf{L}^1$ at 564 nm excitation (only the intermediate pH species is fluorescent) and (B) speciation diagram for the three forms of the free ligand $\mathbf{L}^1$ as a function of pH (structures shown in Scheme 2). The total ligand concentration was 2 μM (in 4:1 H_2O/MeCN). The three points at each pH value correspond to the calculated species distribution (SPECFIT) derived from their fluorescence spectra.

Scheme 2

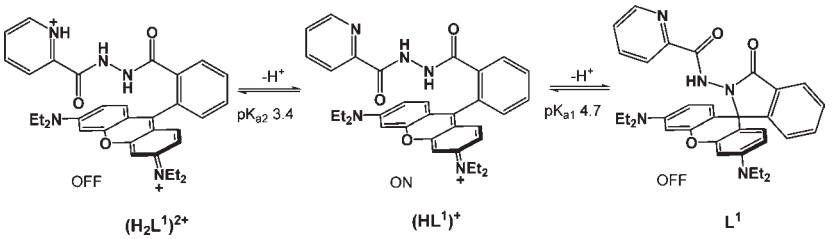

ESI mass spectra were measured on a Bruker HCT 3D Ion Trap spectrometer. Electronic spectra were measured on a Perkin-Elmer Lambda 35 spectrophotometer.

pH-Dependent Fluorescence. The pH dependent fluorescence experiments were performed with a universal buffer, which has been previously described,[25] in addition to 0.1 M $NaNO_3$. The pH of the buffer was adjusted with either 1 M nitric acid or 2.5 M sodium hydroxide. A 2 mL aliquot of of either $\mathbf{L}^1$ or $[Fe(\mathbf{L}^1)_2](ClO_4)_3 \cdot 3H_2O$ solution (10 μM in MeCN) was added to 8 mL of buffer solution. Fluorescence and final pH were measured after 1 h for the ligand and after 10 min for the complex.

Cell Plating. HeLa cells were cultured in DMEM, penicillin−streptomycin−glutamine, and fetal bovine serum medium. One day prior to experiments, cell suspensions were plated on 35-mm-diameter circular glass coverslips. The cells were washed with phosphate buffered saline (PBS, pH 7.4) and then incubated with either 100 nM LysoTracker Green, 40 μM Fe^{3+}, or 80 μM $\mathbf{L}^1$ depending on the experiment, for 30 min in the medium. 0.5% DMSO was used to improve $\mathbf{L}^1$ or $[Fe(\mathbf{L}^1)_2]^{3+}$ solubility. Cells were washed again with PBS prior to imaging.

Microscopy. Cells were imaged on a Nikon A1 confocal laser microscope system, fitted to a Nikon T1 inverted microscope with 100× oil and 20× air objectives. Dyes were excited with lasers at 488 and 561 nm, and emission was collected between 500 and 550 nm and 570 and 620 nm, respectively, or via an integrated a spectrograph. Images were acquired and processed with Nikon NIS Elements software.

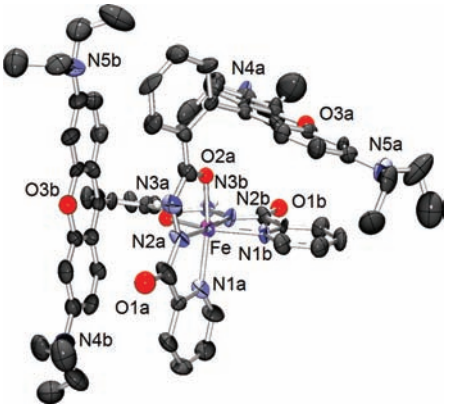

Figure 3. ORTEP view of the $[Fe(\mathbf{L}^1)_2]^{3+}$ cation (30% probability ellipsoids) with alkyl and aryl H atoms omitted. Selected bond lengths (Å): Fe−N1a, 2.115(8); Fe−N1b, 2.108(9); Fe−N2a, 1.995(8); Fe−N2b, 1.973(8); Fe−O2a, 2.019(5); Fe−O2b, 2.021(6).

RESULTS AND DISCUSSION

Synthesis and Characterization of $\mathbf{L}^1$. Ligand $\mathbf{L}^1$ was synthesized from rhodamine B hydrazide[21] via acylation with a

dx.doi.org/10.1021/ic201495r |Inorg. Chem. 2011, 50, 9178–9183

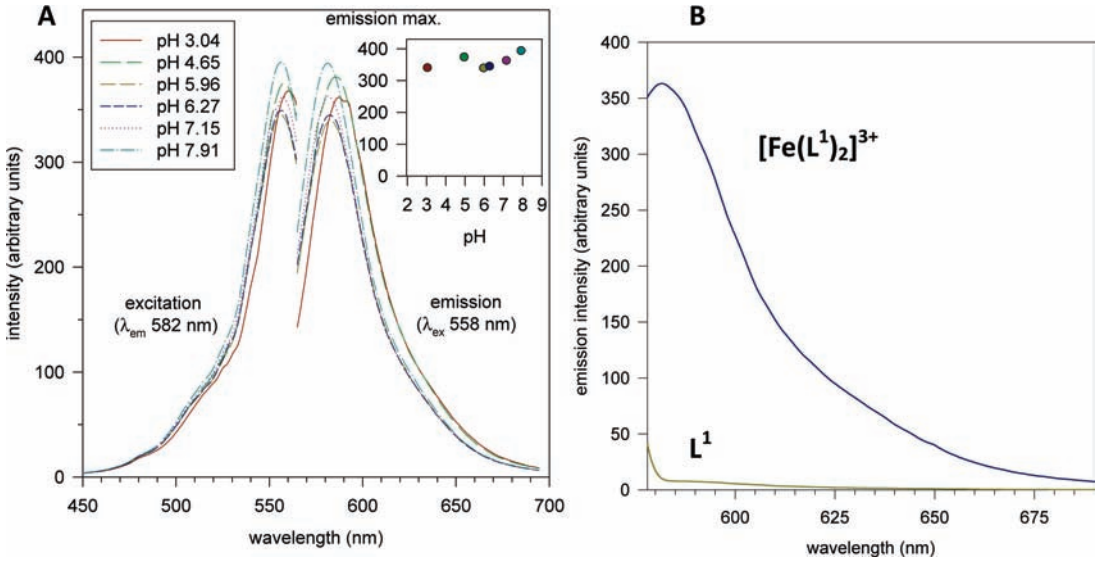

Figure 4. (A) Emission and excitation spectra of $[Fe(L^1)_2]^{3+}$ as a function of pH. Inset: variation of emission maximum intensity with pH (in 4:1 H_2O/MeCN). (B) Fluorescence spectra of the free ligand $\mathbf{L^1}$ (pH 7.0, 564 nm excitation) and the complex $[Fe(\mathbf{L^1})_2]^{3+}$ (pH 7.2, 558 nm excitation). Both solutions contain 2 μM ligand (4:1 H_2O/MeCN).

mixed tosic picolinic anhydride in the presence of *N*-methylimidazole. Under these mild reaction conditions,[26] $\mathbf{L^1}$ was obtained in 62% yield after chromatography on neutral alumina. The crystal structure of $\mathbf{L^1}$ (Figure 1) reveals the spiro lactam configuration (spiro atom C14) with the metal chelating residue orthogonal to the oxo-tricyclic ring system of the rhodamine moiety.

Ring-opening of $\mathbf{L^1}$ may be triggered by metal chelation (see below) or protonation. A pH-dependent fluorescence profile (in 4:1 H_2O/MeCN) was generated with a series of 12 *buffered* solutions of equal total concentration of the ligand. The fluorescence spectra were strongly pH-dependent. The spectra are shown in Figure 2A, and the data were fit to a dibasic acid model where the intermediate monoprotonated form alone is fluorescent (Figure 2B). The two pK_a values at which fluorescence is modulated (pK_{a1} 4.71(1) and pK_{a2} 3.44(1)) were obtained by global analysis of the 12 fluorescence spectra with SPECFIT.[27] At pH 6 and above, the dominant species in solution is the nonfluorescent spiro (ring-closed) form of compound $\mathbf{L^1}$ (Figure 1). The monoprotonated species $[H\mathbf{L^1}]^+$ is assigned to a ring-opened form (Scheme 2), while the doubly protonated (nonfluorescent) $[H_2\mathbf{L^1}]^{2+}$ is protonated at the pyridyl ring by analogy with potentiometric titration data reported for nonfluorescent analogues from this series.[7] It is likely that the pyridinium ring (an electron acceptor) quenches fluorescence by photoinduced electron transfer.[28]

Synthesis and Characterization of $[Fe^{III}(L^1)_2]^{3+}$. $\mathbf{L^1}$ was reacted with ferric perchlorate in ethanol to afford the complex $[Fe(\mathbf{L^1})_2](ClO_4)_3\cdot 3H_2O$ as a dark brown solid. The crystal structure of the complex (Figure 3) confirms the 2:1 ligand/metal ratio of the complex, reminiscent of other diaroyl hydrazine complexes.[6,7] Complexation is accompanied by ring-opening; N3a and N3b are protonated while the picolinamide N atoms (N2a/b) deprotonate and coordinate to the metal, giving a tridentate zwitterionic ligand. The coordinate bond lengths and angles mirror those found for the unsubstituted picolinoyl hydrazine, high-spin complexes of Fe^{III}.[6,7] The bulky planar tricyclic rhodamine moieties are forced into an approximately parallel conformation relative to the *NNO* chelating group of the adjacent ligand (Figure 3).

A typical rhodamine fluorescence spectrum is seen for $[Fe(\mathbf{L^1})_2]^{3+}$ in the pH range 3−8 (Figure 4A). The excitation and emission maxima vary somewhat across this pH range but not in a systematic way (Figure 4A). The fluorescence spectra of $[Fe(\mathbf{L^1})_2]^{3+}$ and $\mathbf{L^1}$ at equal concentrations (2 μM) and at ~pH 7 are compared in Figure 4B, illustrating the "turn-on" fluorescent behavior of $\mathbf{L^1}$ when complexed with Fe^{III}. As a comparison, a similar experiment carried out with Zn^{II} did not turn on fluorescence (Supporting Information).

Confocal Microscopy. The preformed complex $[Fe(\mathbf{L^1})_2](ClO_4)_3$ (40 μM in PBS + 0.5% DMSO) was incubated with HeLa cells for 30 min. After washing the cells, a strong intracellular fluorescence was observed (Figure 5A) characteristic of the $[Fe(\mathbf{L^1})_2]^{3+}$ complex. On the basis of their tubular punctuate form, localization of the complex within endosomes or lysosomes is indicated.[29] This was confirmed by coincubation of $[Fe(\mathbf{L^1})_2]^{3+}$ with the lysosome-specific dye LysoTracker Green DND-26 (Invitrogen), leading to green emission from the same cellular locations (Figure 5B). Emission spectra (at 6 nm resolution) were acquired at the intracellular (red dot) and extracellular (blue dot) locations marked in Figure 5C. The spectra are shown in Figure 5C. The red dots overlay the emission spectrum of $[Fe(\mathbf{L^1})_2]^{3+}$ (black curve in Figure 5D). These experiments confirm that $[Fe(\mathbf{L^1})_2]^{3+}$ is able to enter HeLa cells as an intact complex and that the compound is compartmentalized within lysosomes.

HeLa cells were incubated with free ligand $\mathbf{L^1}$ (80 μM, incl. 0.5% DMSO) for 30 min (Figure 6). Again, the characteristic rhodamine-based fluorescence was seen localized within endosomes or lysosomes of the cells confirming cell penetration by the profluorescent ligand $\mathbf{L^1}$. Although the emission profile is consistent with the formation of $[Fe(\mathbf{L^1})_2]^{3+}$ *in vivo*, through chelation of labile ferric ions, the fluorescence profile is indistinguishable from that of the ring-opened free ligand $(H\mathbf{L^1})^+$. In fact, this ambiguity is a problem inherent to every claimed rhodamine-based metal ion sensor, although this is rarely conceded.

dx.doi.org/10.1021/ic201495r |*Inorg. Chem.* 2011, 50, 9178–9183

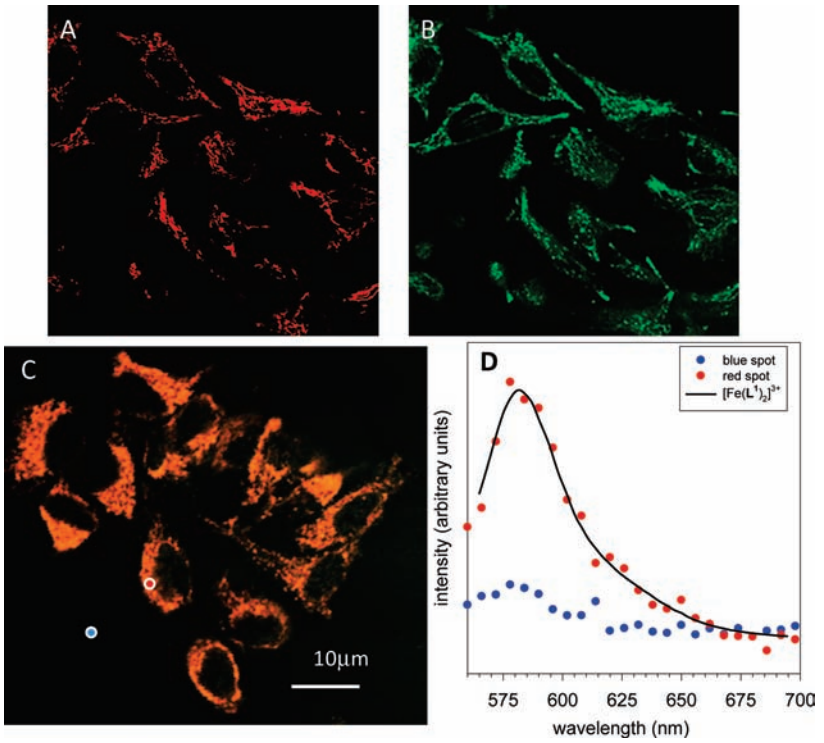

Figure 5. HeLa cells incubated with a solution containing (A) $[Fe(\mathbf{L^1})_2]^{3+}$ 40 μM excited at 561 nm and imaged between 570 and 620 nm and (B) LysoTracker Green excited at 488 nm and imaged between 500 and 550 nm. (C) True color spectral imaging of the HeLa cells incubated with $[Fe(\mathbf{L^1})_2]^{3+}$ excited at 514 nm. (D) Localized spectra at intracellular (red) and extracellular (blue) regions shown in C. The solution-based emission spectrum of $[Fe(\mathbf{L^1})_2]^{3+}$ at pH 7.2 (black line) is included.

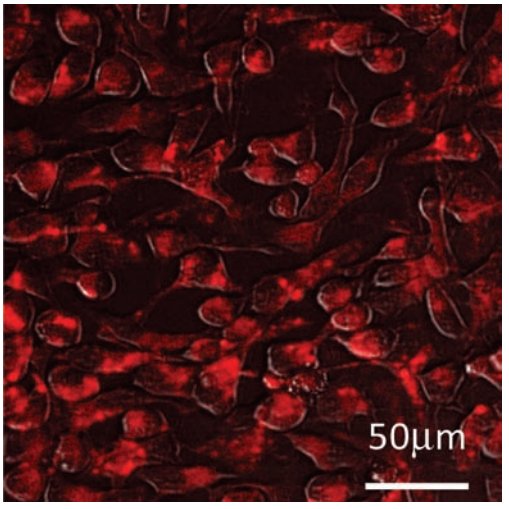

Figure 6. Confocal microscopy image of HeLa cells incubated with $\mathbf{L^1}$ (80 μM) for 30 min.

It is known that lysosomes contain high concentrations of labile Fe[30,31] and their interior is weakly acidic (pH 4−6),[32,33] so either H^+ or Fe^{3+} (both being present) may give a positive fluorescent response.

As noted above, all rhodamine-based compounds[34] are fluorescent at *ca.* pH 5.5 and below due to proton-driven ring opening (Scheme 1). The rhodamine lactam reported by Wang et al.[20] as well as related ligands[17,18] lacking an obvious Fe chelating moiety have all been claimed to function as Fe^{III} sensors. However, no Fe complexes were isolated or characterized in any of these papers. In the absence of properly characterized Fe complexes, doubt remains as to whether the intracellular fluorescent species was indeed an Fe complex.

CONCLUSIONS

In conclusion, we have fully characterized the potentially fluorescent Fe chelator $\mathbf{L^1}$ in its free ligand form and as its Fe^{III} complex $[Fe(\mathbf{L^1})_2]^{3+}$. Both $\mathbf{L^1}$ and $[Fe(\mathbf{L^1})_2]^{3+}$ are able to enter live HeLa cells, and it has been demonstrated that the fluorescent Fe complex localizes within endosomes or lysosomes. However, the intracellular fate of $\mathbf{L^1}$ (as opposed to $[Fe(\mathbf{L^1})_2]^{3+}$) remains unclear. Despite its identical cellular permeability and intracellular localization, discrimination between its fluorescent protonated ($[H\mathbf{L^1}]^+$) or chelate ($[Fe(\mathbf{L^1})_2]^{3+}$) forms *in vivo* requires more sophisticated cell studies, beyond the scope of this work. Control of intracellular (and subcellular) Fe concentrations as well as the lysosomal pH may resolve this issue. Nevertheless, the fluorescent ferric complex $[Fe(\mathbf{L^1})_2]^{3+}$ alone is a major advance on "turn-off" Fe probes (such as calcein) that have been reported in the past. Furthermore, $[Fe(\mathbf{L^1})_2]^{3+}$ represents the first rhodamine-based Fe complex to be properly characterized. Further synthetic work based on both increasing sensitivity and controlling subcellular localization is underway.

ASSOCIATED CONTENT

Supporting Information. Crystallographic data in CIF format and a plot of the relative fluorescence of L^1 brought

dx.doi.org/10.1021/ic201495r |*Inorg. Chem.* 2011, 50, 9178–9183

about by equal concentrations of Fe^{III} and Zn^{II}. This material is available free of charge via the Internet at http://pubs.acs.org.

AUTHOR INFORMATION

Corresponding Author
*E-mail: p.bernhardt@uq.edu.au, jason.davis@chem.ox.ac.uk.

ACKNOWLEDGMENT

P.V.B. and M.J.R. gratefully acknowledge the Australian Research Council for financial support (DP1096029). J.J.D. and M.B. gratefully acknowledge the Biotechnology and Biological Sciences Research Council and Nikon U.K. for support.

REFERENCES

(1) Kalinowski, D. S.; Richardson, D. R. *Chem. Res. Toxicol.* **2007**, *20*, 715–720.
(2) Hider, R. C.; Kong, X. L.; Roy, S.; Ma, Y. M.; Preston, J. *J. Pharm. Pharmacol.* **2010**, *62*, 1369–1370.
(3) Kontoghiorghes, G. J.; Spyrou, A.; Kolnagou, A. *Hemoglobin* **2010**, *34*, 251–264.
(4) Bernhardt, P. V. *Dalton Trans.* **2007**, 3214–3220.
(5) Sharpe, P. C.; Richardson, D. R.; Kalinowski, D. S.; Bernhardt, P. V. *Curr. Top. Med. Chem.* **2011**, *11*, 591–607.
(6) Bernhardt, P. V.; Chin, P.; Richardson, D. R. *J. Biol. Inorg. Chem.* **2001**, *6*, 801–809.
(7) Bernhardt, P. V.; Chin, P.; Sharpe, P. C.; Wang, J.-Y. C.; Richardson, D. R. *J. Biol. Inorg. Chem.* **2005**, *10*, 761–777.
(8) Bernhardt, P. V.; Chin, P.; Sharpe, P. C.; Richardson, D. R. *Dalton Trans.* **2007**, 3232–3244.
(9) Que, E. L.; Domaille, D. W.; Chang, C. J. *Chem. Rev.* **2008**, *108*, 1517–1549.
(10) Esposito, B. P.; Epsztejn, S.; Breuer, W.; Cabantchik, Z. I. *Anal. Biochem.* **2002**, *304*, 1–18.
(11) Domaille, D. W.; Que, E. L.; Chang, C. J. *Nat. Chem. Biol.* **2008**, *4*, 168–175.
(12) Fakih, S.; Podinovskaia, M.; Kong, X.; Collins, H. L.; Schaible, U. E.; Hider, R. C. *J. Med. Chem.* **2008**, *51*, 4539–4552.
(13) Fakih, S.; Podinovskaia, M.; Kong, X.; Schaible, U. E.; Collins, H. L.; Hider, R. C. *J. Pharm. Sci.* **2009**, *98*, 2212–2226.
(14) Breuer, W.; Epsztejn, S.; Cabantchik, Z. I. *J. Biol. Chem.* **1995**, *270*, 24209–15.
(15) Petrat, F.; de Groot, H.; Rauen, U. *Arch. Biochem. Biophys.* **2000**, *376*, 74–81.
(16) Bricks, J. L.; Kovalchuk, A.; Trieflinger, C.; Nofz, M.; Bueschel, M.; Tolmachev, A. I.; Daub, J.; Rurack, K. *J. Am. Chem. Soc.* **2005**, *127*, 13522–13529.
(17) Xiang, Y.; Tong, A. *Org. Lett.* **2006**, *8*, 1549–1552.
(18) Zhang, M.; Gao, Y.; Li, M.; Yu, M.; Li, F.; Li, L.; Zhu, M.; Zhang, J.; Yi, T.; Huang, C. *Tetrahedron Lett.* **2007**, *48*, 3709–3712.
(19) Lin, W.; Long, L.; Yuan, L.; Cao, Z.; Feng, J. *Anal. Chim. Acta* **2009**, *634*, 262–266.
(20) Wang, B.; Hai, J.; Liu, Z.; Wang, Q.; Yang, Z.; Sun, S. *Angew. Chem., Int. Ed.* **2010**, *49*, 4576–4579.
(21) Xiang, Y.; Tong, A.; Jin, P.; Ju, Y. *Org. Lett.* **2006**, *8*, 2863–6.
(22) Sheldrick, G. M. *Acta Crystallogr., Sect. A* **2008**, *A64*, 112–122.
(23) Farrugia, L. J. *J. Appl. Crystallogr.* **1997**, *30*, 565.
(24) Farrugia, L. J. *J. Appl. Crystallogr.* **1999**, *32*, 837.
(25) Avdeef, A.; Tsinman, K. L. Patent WO2001055698A1, 2001.
(26) Wakasugi, K.; Iida, A.; Misaki, T.; Nishii, Y.; Tanabe, Y. *Adv. Synth. Catal.* **2003**, *345*, 1209–1214.
(27) Binstead, R. A. *SPECFIT, Global Analysis System*; Spectrum Software Associates: Marlborough, MA, 2007.
(28) Laine, P. P.; Campagna, S.; Loiseau, F. *Coord. Chem. Rev.* **2008**, *252*, 2552–2571.
(29) Shi, H.; He, X.; Yuan, Y.; Wang, K.; Liu, D. *Anal. Chem.* **2010**, *82*, 2213–2220.
(30) Kurz, T.; Gustafsson, B.; Brunk, U. T. *FEBS J.* **2006**, *273*, 3106–3117.
(31) Yu, Z.; Persson, H. L.; Eaton, J. W.; Brunk, U. T. *Free Radical Biol. Med.* **2003**, *34*, 1243–1252.
(32) Van Dyke, R. W.; Belcher, J. D. *Am. J. Physiol. Cell Physiol.* **1994**, *266*, C81–C94.
(33) Schindler, M.; Grabski, S.; Hoff, E.; Simon, S. M. *Biochemistry* **1996**, *35*, 2811–2817.
(34) Zhang, W.; Tang, B.; Liu, X.; Liu, Y.; Xu, K.; Ma, J.; Tong, L.; Yang, G. *Analyst* **2009**, *134*, 367–371.